VOL. 12, NO. 15, AUGUST 2017 ISSN 1819-6608
ARPN Journal of Engineering and Applied Sciences

www.arpnjournals.com

DELETION OF THE MIR-145 TARGET SEQUENCE AND ELIMINATING THE REPRESSION OF MEIS1 EXPRESSION DURING THE ZEBRAFISH HEMATOPOIESIS

Nibras Najm Abbood and Amir Abdullah Jabir
Department of Marine Vertebrate, Marine Sciences Centre, University of Basra, Basra, Iraq
E-Mail: nibras.abbood@gmail.com

ABSTRACT

Matured miRNAs are stimulated from elongated endogenous principal transcripts by the RNase III enzymes, Drosha and Dicer resulting in 22-nt double-stranded RNAs. One single strand of the duplex develops accumulated into the RNA-induced silencing complex (RISC) coincident with target identity and coupling. MiRNAs provide a smart mechanism that offers exceptionally tuned control of protein levels by adjusting translational efficacy and mRNA power. In this research work, we convey that zebrafish embryos having reduced function of the orthologous hoxd4a gene clear striking perturbations in vasculogenesis, angiogenesis and primitive and definitive hematopoiesis. These defects are headed by condensed expression of the hemangioblast markers scl1, lmo2 and fli1 inside the posterior lateral plate mesoderm (PLM) at 13 hours post fertilization (hpf). Epistasis analysis clearly shown that hoxd4a acts upstream of meis1.1 but downstream of cdx4 as initial as the shield stage in ventral-most mesoderm fated to grow to hemangioblasts, leading us to suggest that loss of hoxd4a function disturbs hemangioblast requirement. These results place hoxd4a higher in a genetic hierarchy leading hemangioblast formation downstream of cdx1/cdx4 and upstream of meis1.1. An added significance of impaired hoxd4a and meis1.1 expression is the deregulation of multiple Hox genes involved in vasculogenesis and hematopoiesis which may additionally subsidize to the defects labelled here. In this paper, the deletion of the miR-145 target sequence and eliminating the repression of meis1 expression during the zebrafish hematopoiesis has been vividly elaborated.

Keywords: zebrafish, target sequence, hematopoiesis, MicroRNA, mesoderm.

1. INTRODUCTION

The original miRNA (lin-4) was revealed in 1993 and meanwhile then, hundreds if not thousands of miRNAs have been recognized and combined with several databases comprising of (miRNA.org and MirBASE.org). Accepting the purpose of miRNA stems from escalating their production, which commences with the transcription of primary transcripts referred as pri-miRNAs by RNA polymerase II. Pri-miRNAs typically extends from hundreds to thousands of nucleotides in length, and so must experience three cleavage steps afore their activation to control genes. Handling begins in the nucleus by the usage of ribonuclease the Drosha and DGCR8 (DiGeorge syndrome critical region 8) complex to develop as an intermediary hairpin referred as a pre-miRNA of around 70-100 nucleotides in length. The pre-miRNA is elated out of the nucleus by exportin-5 and transported to the cytoplasm to be transformed to an 18-25 nucleotide, subsequently mature double-stranded miRNA is treated using a ribonuclease referred as Dicer. Successively, the miRNA double-strand is detached to offer a mature, active miRNA by the usage of an effector complex called as RNA-induced silencing complex (RISC). Subsequent to the creation of this mature miRNA, the explicit complementary region of the 3' untranslated region (UTR) of a messenger RNA (mRNA) could be targeted. By combining the mRNA and miRNA, the RISC complex persuades deprivation of the double-stranded mRNA. Additional probable contrivance that miRNAs use is the blocking of protein translation procedures, consequently ensuing in the eradication of that explicit protein that is being conveyed. Inspection of tumour-specific miRNA expression profiles has exposed that miRNAs could be the master regulators of numerous features of tumour biology and many research works have revealed that miRNA themselves can fpartake the role as tumour suppressor genes or oncogenes, where gene repression or over expression can have a diagnostic and prognostic implication [12]. Up regulation of oncogenic miR-17 by cMyc was revealed to disturb cell cycle control mechanisms and to interrupt the apoptotic regulator E2F1. Succeeding these significant detections in 2005, numerous correlations amongst miRNA expression, with Weinberg's six hallmarks of cancer have been recognized. Regardless of the heave in epigenetic investigation in the last few decades, the characters of miRNA in numerous human cancers such as leukaemia and lymphoma have not been obviously well-defined. Manipulation of miRNA regulation could be an innovative method to achieve an idea for the regulatory methodologies of miRNA in cancer [1]. Alterations in the expression of a quantity of transcription factors have been related with various blood cancers, with irisingindication supporting a character for the regulation of transcription factors by the miRNAs. The cardiovascular structure is the basic organ system that generally grows during embryogenesis, and is indispensable for embryo feasibility and existence. MiRNAs are also extremely uttered in the cardiovascular system; though, their biological characters in the mammalian cardiovascular system have only been clarified meanwhile in 2005. Numerous researches have confirmed that miRNAs [9] play significant characters not

only in the cardiovascular development, but also in the cardiovascular disease [14, 16, 21].

2. MEIS1 IN STANDARD HEMATOPOIESIS

Meis1 is one of the most extremely preserved transcription factors in hematopoiesis with more than 90% amino acid sequence homology amongst the zebrafish and other vertebrates. They abused this high level of conservation and that of other crucial regulators of hematopoiesis, e.g. scl, gata1 and gata2, and evaluated the consequence of morpholino (MO) knockdown of zebrafish meis1 on progenitor and hematopoietic stem cell development process. Additionally, they have carried out research works on the growth of the vascular system where angiogenesis and remodeling processes are accountable for the development of a functional circulatory system and stem cell niches. In current years, examinations into the origin of Leukemia stem cells (LSCs) have discovered that these cells are amazingly analogous to normal Hematopoietic stem cells (HSCs), with respect to their capability to self-renew, cell surface markers and differentiation capabilities [3].

Therefore, it is believable and most probable that *Meis1*shows a crucialpart in normal HSC biology as well. Numerous additional lines of confirmation specify that this may be the usual case. First, *Meis1*, along with *Hox* genes are co-expressed in the most primeval hematopoietic subpopulations and are down-regulated following the differentiation. Second, Meis1-deficient mice expire by embryonic day 14.5, bestowing with widespread hemorrhaging due to the deficiency of megakaryocytes. While conclusive myeloerythroid lineages are present in these embryos, the overall quantities of colony-forming cells are suggestively abridged. *Meis1*$^{-/-}$ fetal liver cells miscarry to radio protect fatally exposed recipient mice and they contest unwell in repopulation analyses even though they provision the creation of all hematopoietic lineages [4]. It is conceivable that gene redundancy amongst the meticulously related *Meis* family members could recompense for the loss of *Meis1*, and therefore may avoid the whole retraction of HSC action in these mice. Taken together, these readings offer robust sustenance for the hypothesis that *Meis1*shows an imperative character in the HSC self-renewal/proliferation.

Above the years, the zebrafish has established its appropriateness as a prototypical system for advancing our understanding of the genetic rule of hematopoiesis in both normal and pathological states. As in mammals [18], primitive and definitive hematopoiesis happens in zebrafish in structurally dissimilar locations and can be further discriminated on the basis of cell types fashioned. Primitive hematopoiesis yields primitive macrophages, which originate from cephalic mesoderm, and primitive erythrocytes originate from the intermediate cell mass (ICM).However, definitive hematopoiesis offers first to erythromyeloid progenitors in the posterior blood island and thereby to hematopoietic stem cells in the aorta-gonad-mesonephros (AGM) location, from the generation spot in the AGM, hematopoietic stem cells move to the caudal hematopoietic tissue, where they enlarge and lastly touch the pronephros and thymus, thus resolving in their ultimate destination, the stem cell niches.

As HOXA9 and MEIS1 partake important developmental characters, are collaborating DNA binding proteins and leukemic oncoproteins, and are typically imperative for standard hematopoiesis, the regulation of Meis1 by its companion protein is of interest [20]. Loss of Hoxa9 produced down regulation of the Meis1 mRNA and protein, while forced HOXA9 expression up regulated Meis1. Hoxa9 and Meis1 expression was associatedwith the hematopoietic progenitors and severe leukemia. Meis1+/− Hoxa9−/− deficient mice, created to test HOXA9 regulation of endogenous Meis1, were unimportant and had abridged bone marrow. These information specify that HOXA9 modulates Meis1 during standard murine hematopoiesis [5, 13].

3. ZEBRAfiSH (DANIO RERIO) AS A MODEL ANIMAL

It is an outstanding model organism to learn both developmental and physiological procedures, due to the familiar series of distinguishing features, containing its sequenced genome. There are more benefitsin using zebrafish as a model animal. Zebrafish typically became one of the most prevalent and well-established models in genetics and developmental biology due to its small life cycle, minor size, and comfortin laboratory maintenance. This sorted out zebrafish as an expedient model in cancer research including chemical carcinogenesis [2, 7, 8, 11].

Zebrafish has also developed the emphasis of a foremost research exertion into indulgentto the molecular and cellular events which command the development of vertebrate embryos. Similarly, the zebrafish has demonstrated good-looking in studies scrutinizing the factors which upset the formation of transgenic fish and the expression of transgenes [17]. The developments which have been made in these regions have determinedly established this trivial aquarium fish as a foremost model system in biological and biotechnological research [6].

4. MATERIALS AND METHODS

4.1. Antisense morpholino and mRNA microinjection

The Antisense morpholino oligonucleotides (MOs) were attained from Gene Tools Inc and inoculated into zebrafish embryos at 1-4 cell stage [10]. Splice MOs targeting the 5′ splice site intron-exon junction (splice acceptor) are selected as follows: MO1:5′-GTT CAC TGT GAA GGA CAA AAT CAC A-3′ and exon-intron junction (splice donor), MO2:5′- GCA AAG AGA GTG GAT CTT ACC CGT A-3′. MOs were adulterated in Danieau's buffer (0.4 mM $MgSO_4$, 0.6 mM $CaCl_2$, 0.7 mMKCl, 58 mMNaCl, and 5 mMHepes, pH 7.6). Optimal quantities for each MO were verified based on phenotypic effects, and every experiment was executed in analogous manner with a non-specific MO (standard control MO delivered by GeneToolsInc) injected at the similar attention. Full-length cDNA for *hoxd4a* was created by PCR using the primers and cloned into pCR®II-TOPO®. The mMESSAGEmMACHINE Kit (Ambion) was

employed to produce capped mRNA. All mRNAs used for release experiments were evaluated over a range of

4.2. Whole mount in situ hybridization and imaging

The whole mount *in situ* hybridization (WISH) was achieved as defined earlier. For *nkx2.5*, a PCR section was intensified from 26–28 hpf embryonic cDNA by using the primers. The reverse primer assimilated a T7 promoter permitting the PCR product to be employed openly for probe production. DIG- labeled antisense RNA probes were transcribed from linearized template by using the T3, T7 or SP6 RNA polymerase (Roche). Probes for *hoxb6b* and *hoxb7a* has been derived by the RT-PCR-mediated amplification from RNA from 26-28 hpf embryos btusing the primers termedby Wan et al. Embryos were hatched with anti-DIG antibody (Roche) and probes were noticed using NBT/BCIP (nitro blue tetrazolium chloride/5-bromo-4-chloro-3-indolyl phosphate, toluidine salt) from Roche. Images were acquired on a Zeiss lumar V.12 stereo microscope with an Axio Cam MRc (Zeiss) and Axio Vision software. Few embryos were then dismembered away from the yolk and flat-mounted former to the photography.

4.3. Alkaline phosphatase staining of blood vessels

Embryos at 72 hpf were attached with 4% paraformaldehyde in PBS (phosphate buffered saline) at a normal room temperature for 30 minutes, followed by the treatment with pre-cooled acetone for 30 minutes at -20°C. Subsequently rinsing with PBS twice (5 minutes each), the embryos were equilibrated with NTMT buffer (100 mMTris pH 9.5, 50 mM $MgCl_2$, 100 mMNaCl, 0.1% Tween 20) for three times (each for 15 minutes) at normal room temperature. For alkaline phosphatase staining, the embryos have beenhatched in NBT/BCIP (Roche) solution for 30 minutes.

4.4. O-dianisidine staining

Staining with o-dianisidine has beendone as described in the preceding sections. Control and MO-injected embryos at 48 and 72 hpf were physically dechorionated and fixed with 4% paraformaldehyde overnight. Fixed quantity of embryos were washed three times in PBS and then hatched in the staining buffer (0.6 mg/ml o-dianisidine, 10 mM sodium acetate (pH 5.2), 0.65% hydrogen peroxide, and 40% ethanol) for 15 minutes in the dark. Stained embryos were unfurnished and stored in benzyl benzoate/benzyl alcohol (2:1, vol/vol).

4.5. Flow cytometry

Control- and morpholino-injected Tg(gata1:dsRed) embryos (150 embryos each) were dechorionated physically at 48 hpf, rinsed for 15 minutes in calcium-free Ringer's solution and passed five times through a 200 µl pipette tip to eliminate the yolk. The embryos were detached in 0.25% trypsin and 1 mM EDTA for 60 minutes at 28.5°C, during which the sample was passed six times through a 200 µl pipette tip every 10 minutes so as to acquire a single cell suspension. The dissociated cell suspension was centrifuged at 1000 g for 9 minutesat 4°C, the supernatant being discarded, and the cells resuspended in ice cold 0.9× PBS plus 5% fetal bovine serum and passed by gravity through a 40 µm nylon mesh filter. Flow cytometry has been done on a BD LSII instrument (BD Biosciences) [23].

5. RESULTS

5.1. MiR 142-3P is expressed during zebrafish early developmental stage

We used RT-PCR (Reverse Transcription PCR) to investigate the expression of miRNA 142-3p throughout zebrafish early developmental stages as indicated in figure1, a fragile expression was at the early stages [1 cell, 16 cells, 512 cells, Oblong, 5.3 h (50% epiboly), 12 h (6 somite)] and robust expression at 24 hpf and 48 hpf respectively.

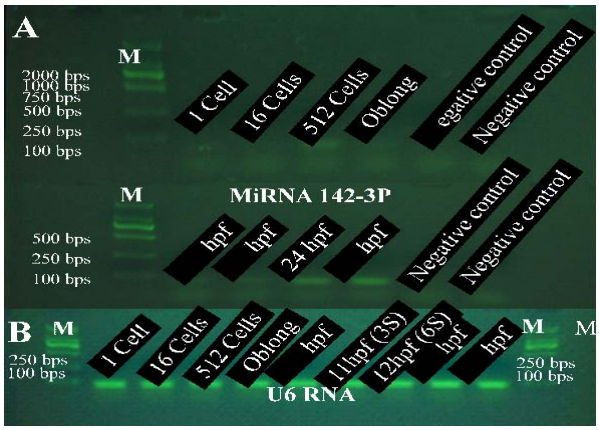

Figure-1. RT-PCR (Reverse Transcription PCR) for zebrafish developmental stages exhibited that (A) miR142-3p expression was not so robust in former stages [1 cell, 16 cells, 512 cells, oblong, 5.3 hpf (50% epiboly) and 12 hpf (6 somite)] but it was so robust in 24 hpf and 48 hpf stages, when associated with (B) U6RNA RT-PCR result, M is Trans2K DNA Marker (DNA MASS 5µl) [19].

5.2. MiR-142-3P is essential for erythoid formation repression and myeloid expansion in zebrafish

To identify whether miR142-3p has a character in erythroid cells development and myeloid expansion, we employed O-dianisidine staining for 48 hours, 72 hours and 96 hours post fertilization injected embryos (with Agomir142-3p, Antagomir142-3p). In regulator embryos, erythropoiesis development was with usual quantity. For 48 hpf injected embryos with Agomir142-3p, there was a noteworthy reduction in erythropoiesis (blood formation) (more than 90% (n=60) of injected embryos with agomir142-3p had strong reduction in erythropoiesis in the yolk sacarea) and around 88% (n=54) of injected embryos with Antagomir142-3p had strongupsurge in erythropoiesis formation in the yolk sac area), because of Antagomir 142-3p caused block for agomir142-3p

expression, so it exhibited upsurge for erythropoiesis creation (increased blood formation) as a normal as displayed in Figure-2. And for 72 hpf injected embryos, we have perceived that Agomir142-3p also produced reduction with blood formation and Antagomir142-3p produced increase with blood formation as exhibited in figure 2, nevertheless an effect for both of them was fewer than their effect in 48 hpf injected embryos (about 58% of injected embryos with agomir142-3p had decrease and 62% of injected embryos with Antagomir142-3p had increase in erythropoiesis formation), and also for 96 hpf injected embryos an outcome of Agomir142-3p and Antagomir142-3p was less than 48 hpf and 72 hpf injected embryos for erythropoiesis creation.

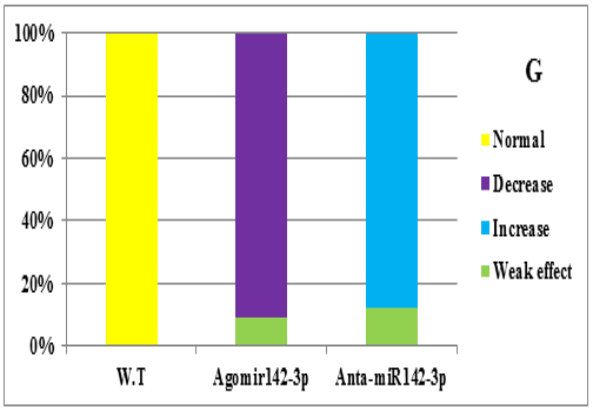

Figure-2. Results of O-dianisidine staining for 48 hpf of zebrafish injected embryos, (A, D) control, (B, E) agomir142-3p over expression exhibited strong reduction in hematopoiesis in yolk sac area, and (C, F) antagomir142-3p knockdown agomir142-3p expression to display upsurge in hematopoiesis, associated with (A, D). (G) O-dianisidine staining percentage of 48 hpf of zebrafish injected embryos, agomir142-3p over expression exhibited more than 90% of injected embryos had reduction (n=60), antagomir142-3p exhibited about 88% of injected embryos had increase (n=54), more than 97% of wild type embryos were usual (n=75).

5.3. Expression pattern of hoxd4a

The expression of *hoxd4a* throughout zebrafish development was observed by WISH. Maternal transcripts were understood at the 1 cell stage, and zygotic transcripts were enthusiastically noticed from 3 hpf to 48 hpf (Figure-3A-G, I, L) and in a bulk of cells till at least 75% epiboly (8-9 hpf) (Figure-3D). An anterior expression border in neurectoderm is noticeable by 10 hpf (bud stage; data not shown) with additional resolution of the border amongst rhombomeres 6 and 7 (r6/7) by 12 hpf (Figure-3E). As perceived before, at 26-28 hpf *hoxd4a* is expressed in the hindbrain with an anterior border at r6/7, in neural crest migrating to the future branchial arches, and in the pectoral fin fields (Figure-3F). We also perceived *hoxd4a* transcripts in the PBI. At no point were *hoxd4a* transcripts detected in the PLM or ICM of control embryos. By 48 hpf, *hoxd4a* expression was deceptive in the AGM and in patches in the area of the caudal vein plexus.

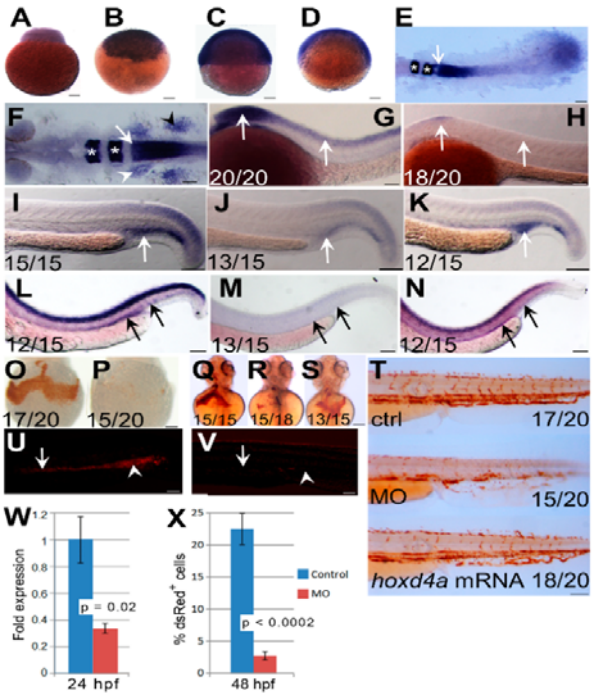

Figure-3. Expression pattern of *hoxd4a* and phenotype of *hoxd4a* morphants. (A–D) Detection of *hoxd4a* transcripts in premature zebrafish embryos [15]. Animal pole is to the top. (A) 1 cell. (B) 3 hpf. (C) 50% epiboly. (D) 75% epiboly. (E) Dorsal view of flat-mounted embryo at 12 hpf (5–6 somites) particularly stained for expression of *hoxd4a* and *krox20a*. The arrow specifies the anterior expression border of *hoxd4a*, whereas asterisks signify expression of *krox20a* in r3 and r5. Anterior is to the left. The rostral-most portion of the embryo is not seized in the image. (F) Dorsal view of a flat-mounted embryo at 26-28 hpf (>26 somites) displaying *hoxd4a* expression in hindbrain, branchial arches (white arrowhead, left side only) and pectoral fin field (black arrowhead, right side only). The white arrow marks the *hoxd4a* anterior expression border in the hindbrain at the boundary amongst r6 and r7. Asterisks denote *krox20a* expression in r3 and r5. (G–H) Lateral views of 26–28 hpf embryos displaying *hoxd4a* expression in the central nervous system (arrows) of control embryos (G) and abridged expression in *hoxd4a* morphants (H). (I-K) *hoxd4a* expression in the caudal half at 26-28 hpf as exposed in lateral views, anterior to the left. *hoxd4a* expression understood in the PBI of control embryos (I, white arrow) is significantly abridged in *hoxd4a* morphants (J). Expression is released following co-injection with capped *hoxd4a* mRNA (K). (L–N) Results of *In situ* hybridization for *hoxd4a* at 48 hpf displaying expression in the AGM and caudal vein plexus (site of future CHT) of control injected embryos (L, black arrows), significantly abridged expression

in *hoxd4a* morphants (M), and released expression in embryos instantaneously injected with capped mRNA for *hoxd4a* (N). (O–T) Hemoglobin within RBCs revealed by o-dianisidine staining. Ventral views at 48 hpf (O,P) and 72 hpf (Q,R) display significantly abridged levels of hemoglobin in the ducts of Cuvier in *hoxd4a* morphants (P and R) vs controls (O and Q). Co-injection with capped mRNA for *hoxd4a* consequences in rescued RBC production (S). (T) O-dianisidine staining of the caudal half of a control larva (upper panel) and *hoxd4a* morphant (middle panel) displaying total decrease in hemoglobin levels at 72 hpf in morphants, and rescue by co-injection of capped *hoxd4a* mRNA (lower panel). (U,V) Lateral visions of trunk areas of Tg(gata1:dsRed) embryos at 26 hpf, anterior to the left side. The expression of dsRed within proerythroblasts is enthusiastically noticed in the ICM (arrow) and PBI (arrowhead) of control-injected embryos (U) but not *hoxd4a* morphants (V). Scale bars=100 µm. Ratios specify the quantity of embryos displaying the presented phenotype. (W) qRT-PCR displays an inclusive 3-fold reduction of *hoxd4a* expression in morphants at 26–28 hpf. Error bars=standard error. p=0.02. (X) Quantitation by flow cytometry of dsRed-positive cells in Tg(gata1:dsRed) embryos at 48 hpf displaying that morphants parade an 88% reduction in RBCs relative to control-injected embryos. Error bars=standard deviation. p<0.0002.

5.4. Loss of hoxd4a impairs definitive hematopoiesis

Between 26 to 30 hpf, definitive hematopoiesis creates at the ventral wall of the DA, with expression of *runx1* and *cmyb* marking the HSCs. The expression of *runx1* and *cmyb* in *hoxd4a* morphants at 26-28 hpf **(**Figure-4A-B vs C-D) and 48 hpf **(**Figure-4E–F vs G-H**)** was harshly down-regulated. The expression levels of markers of primitive and definitive hematopoiesis were evaluated by qRT-PCR and revealed a robustdecrease in *hoxd4a* morphants and noteworthy rescue upon co-injection with capped *hoxd4a* mRNA **(**Figure-4I**)**. Thus, the knockdown of *hoxd4a* results in the impairment of both primitive and definitive hematopoietic lineages.

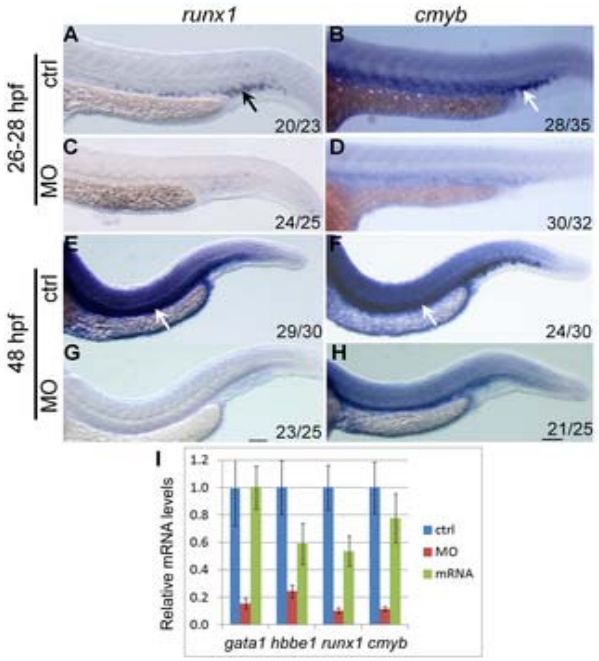

Figure-4. H*oxd4a* expression is essential for transient and definitive hematopoiesis. *In situ* hybridization on 28 hpf (A-D) and 48 hpf (E-H) embryos displaying expression of *runx1* (A, C, E, G) and *cmyb* (B, D, F, H) in probable HSCs arising in the PBI (arrows in A and B) and AGM (arrows in E and F). Expression of both genes was harshlyabridged in *hoxd4a* morphants (C, D and G, H). Ratios in the bottom right corner of images specify the segment of embryos displaying the existing phenotype. ctrl, embryos inserted with a non-specific morpholino. MO, embryos inserted with the anti-*hoxd4a* morpholino. *hoxd4a* mRNA, embryos instantaneously injected with the anti-*hoxd4a* MO plus capped mRNA for *hoxd4a*. Scale bars equal 100 µm. Every images are at the same magnification. (I) qRT-PCR approves the robust depletion of hematopoietic gene expression in *hoxd4a* morphants at 26-28 hpf, and reestablished expression following co-injection with capped mRNA for *hoxd4a*. Samples were standardized to β-actin. Error bars specify standard error. By assessment to controls and rescuants, the gene expression levels of all morphants were statistically dissimilarto p≤0.02 excluding for *gata1* control vs morphant (p=0.04) and *hbbe1* rescuant vs morphant (p=0.09).

5.5. Knockdown of hoxd4a disrupts endothelial development

In addition to abridged quantities of blood cells, *hoxd4a* morphants seemed to lack a normal vasculature. At 48 hpf, blood cells circulated usually in the axial vessels and tail region in control embryos, however in *hoxd4a* morphants, petite or no blood flow could be detected or was extremely unequal with RBCs seeming to become blocked in their path through the ISVs. Blood flow was powerfully released by co-injection with capped *hoxd4a* mRNA. The state of the vasculature

in *hoxd4a* morphants was examined with the use of the *fli1*: EGFP transgenic line which expresses improved GFP under the control of the *fli1* locus in endothelial cells. Whereas control embryos at 72 hpf showed normal vascular phenotypes with the creation of primary ISV joining the dorsal longitudinal anastomotic vessel (DLAV) **(**Figure-5A-B**)**, their morphant counterparts exhibited brutally decreased sprouting of ISV precursors and significantly destabilized GFP signal from the region of the presumptive DA (Figure-5C-D**)**. In around a fifth of morphant embryos, the caudal vein plexus was substituted by an amorphous mass of endothelial tissue **(**Figure-5E–F), while anterior bifurcation of the presumptive aortic vessel might not be detected in others.

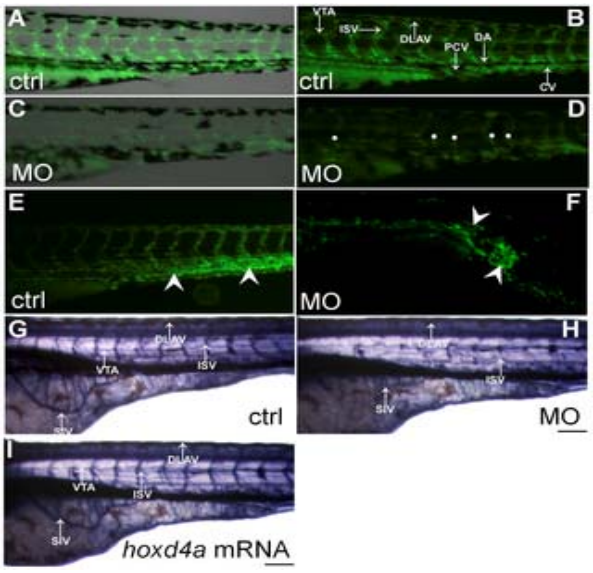

Figure-5. Loss of *hoxd4a* function impairs the development of vasculature. (A–D) Fluorescent images of the trunk and tail regions of Tg (*fli1*: EGFP) embryos at 48 hpf. The panels existent merged bright field and fluorescent images (A,C) or fluorescent images only (B,D) The standard pattern of the vasculature (A,B) is brutally disturbed in *hoxd4a* morphants (C,D) Dorsal extremities of ISV sprouts that fail to exchange the DLAV are marked by white dots (D). The caudal vein plexus of control embryos (E, arrowheads) is substituted by a disorganized quantity of endothelial tissue in *hoxd4a* morphants (F, arrowheads). (G–I) Alkaline phosphatase staining at 72 hpf revealing the vasculature in (G) control-injected larvae, (H) *hoxd4a* morphants, and (I) released larvae co-injected with capped mRNA for *hoxd4a*. Dorsal aorta (DA), posterior cardinal vein (PCV), inter-segmental vessels (ISV), caudal artery (CA), dorsal longitudinal anastomotic vessel (DLAV), caudal vein (CV) and vertebral artery (VTA). All images display lateral views, with frontal to the left and dorsal on top. Scale bars equal 100 µm. $p<0.0002$.

5.6. A Role for hoxd4a in Hemangioblast formation through regulation of meis1.1

The hemangioblast is the usual precursor to the blood and endothelial lineages and is well-defined by the early expression of such genes as *fli1*, *scl1* and *lmo2* in both the ALM and PLM, and *gata5* in the ALM only. The severe flaws in both blood and endothelial lineages in *hoxd4a* morphants recommended that the hemangioblast itself may be negotiated. To evaluate this knowledge, the expression of hemangioblast markers *scl1* and *lmo2* was examined by *in situ* hybridization. Noteworthy down-regulation of both genes was detected in morphants at 13 hpf **(**Figure-6A-B vs C-D**)**. The impaired expression of *scl* and *lmo2* persisted at 26 hpf, signifying that their later independent functions in definitive hematopoiesis were also could be negotiated. Co-injection of capped *hoxd4a* mRNA rescued *scl* and *lmo2* expression at 13 hpf **(**Figure-6E-F**)** and 26 hpf.

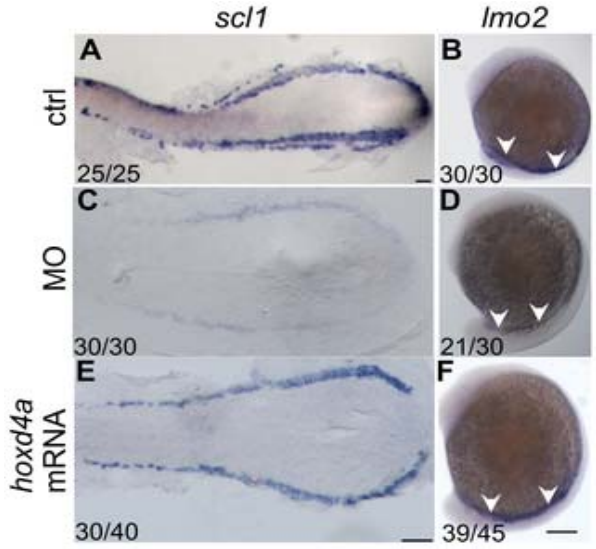

Figure-6. H*oxd4a* is required for hemangioblast creation. (A, B) Normal expression at 13 hpf of posterior hemangioblast markers *scl1* (A) and *lmo2* (B) in the PLM. (C, D) Expression of these markers is significantly abridged in *hoxd4a* morphants, but is released by co-injection of capped mRNA for *hoxd4a* (E, F). Ratios specify the segment of embryos displaying the existing phenotype. Anterior is to the left. A, C and E are dorsal views of flat-mounted specimens while B, D and F are lateral views. Scale bars equal 100 µm. A is at a lesser magnification than C and E.

6. DISCUSSIONS

This research workseats *hoxd4a* near the top of a regulatory cascade directing hematopoiesis, vasculogenesis and angiogenesis in the zebrafish embryos. This unanticipated character of *hoxd4a* is at least partially due to its positive regulation of *meis1.1*, and is probable to have both direct and indirect significances. Most unswervingly, decreased *hoxd4a* function leads to

abridged expression of *meis1.1* in the ventral-most presumptive mesoderm of the shield-stage embryo, a tissue fated to yield the hemangioblast in addition to unipotential erythrocytic and endothelial progenitors. A few hours late, hemangioblast markers are strictly reduced in the PLM, leading us to suggest that *hoxd4a* and *meis1.1* loss of function at the shield stage hinders with the specification of hemangioblasts and unipotential progenitors. Less directly, *hoxd4a* knockdown leads to enormous deregulation of *Hox* gene expression, including a quantity of *Hox* genes previously implicated in these procedures such as *hoxb4a*, *hoxb6b*, *hoxb7a* and *hoxa9a*.

In support of this model, injection of capped mRNA for moreover *hoxd4a* or *meis1.1* rescues principally all the characteristics of the knockdown phenotype. It is likely that much of the consequence of the loss of *meis1.1* expression shadows from the reduced function of MEIS-PBX and MEIS-PBX-HOX transcriptional complexes, however functions of MEIS that are independent of HOX or PBX should also be unnatural. Three reports designate the effects of *meis1.1* loss of function on hematopoiesis and vasculogenesis in zebrafish embryos. Only Ouwehand and co-workers perceived, as we do, defects in both the procedures. Suzuki and co-workers observed defects in the vasculature, heart edema and weakened heartbeat subsequent from decreased *meis1.1* function, and involved a downstream impairment in *flk1* and *vegf* expression, consistent with our findings. Waskiewicz and co-workers observed that loss of *meis1.1* function produced unadorned flaws in erythropoiesis, but did not perceive vasculature flaws nor notice modifications in either *flk1* or Hox expression. Together, these results recommend that the complement of defects we perceive in this study are probable to surpass what can be explained by a simple loss of *meis1.1* function. A full explanation of the phenotypes reported here will likely have to deliberate the roles of *meis1.1*, *hoxd4a* itself, and the downstream effects on the expression of multiple *Hox* genes.

The phenotype we account here is in some ways nearer to that described for *cdx1* plus *cdx4* double loss-of-function embryos, comprising severe hematopoietic (both primitive and definitive) and vasculogenic defects, and reduced expression of multiple *Hox* genes. Some of the phenotypic flaws observed here can be elucidated by effects on comparatively early embryonic events, such as reducedcreation and function of hemangioblast precursors, as designated by the loss of hemangioblast markers *scl*, *lmo2* and *fli1*, and the capability of the capped mRNAs for these genes to release development. Nevertheless, other characteristics of the phenotype may signify later and significantly more downstream functions. For instance, reduced expression of *efnb2a* points to a defect in arterial specification downstream of hemangioblast formation and function, as has been noted in *meis1.1* morphants. Similarly, abundant of the vasculogenic and angiogenicflaws could be elucidated by the impairment of the downstream roles of *fli1, vegf* and *flk1* in these processes. The *vegf* gene is also recognized to play a character in the commencement of hematopoiesis, and its down regulation is consequently probable to subsidize to numerous features of the phenotype reported here [22].Nonetheless, our outcomes highlight the significance of Hox gene function in the early peri-gastrulation phase.

7. CONCLUSION AND FUTURE WORKS

MiRNAs provide an elegant mechanism that contributes excellently tuned control of protein levels by adjusting translational efficacy and mRNA strength. Here, we account that zebrafish embryos having reduced function of the orthologous hoxd4a gene manifest outstanding perturbations in vasculogenesis, angiogenesis and primitive and definitive hematopoiesis. These flaws are headed by abridged expression of the hemangioblast markers scl1, lmo2 and fli1 within the posterior lateral plate mesoderm (PLM) at 13 hours post fertilization (hpf). Epistasis examination exposed that hoxd4a acts upstream of meis1.1 but downstream of cdx4 as early as the shield stage in ventral-most mesoderm fated to give rise to hemangioblasts, leading us to suggest that loss of hoxd4a function disturbs hemangioblast specification. These discoveries place hoxd4a high in a genetic hierarchy directing hemangioblast formation downstream of cdx1/cdx4 and upstream of meis1.1. An added significance of impaired hoxd4a and meis1.1 expression is the deregulation of multiple Hox genes occupied in vasculogenesis and hematopoiesis which may further subsidize to the defects described here. In this paper, the deletion of the miR-145 target sequence and eliminating the repression of meis1 expression during the zebrafish hematopoiesis has been particularized.

REFERENCES

[1] Sheng Qin, *et al.* 2015. Gene regulatory networks by transcription factors and microRNAs in breast cancer. Gene regulatory networks. 31(1):76-83.

[2] Colles Price, *et al.* 2014. MicroRNAs in cancer biology and therapy: Current status and perspectives. Genes & Diseas. 1(1): 53-63.

[3] Ciau-Uitz, A., F. Liu, *et al*. Genetic control of hematopoietic development in Xenopus and zebrafish. Int J Dev Biol. 54(6-7): 1139-1149.

[4] Murayama, E., K. Kissa, *et al*. 2006. Tracing hematopoietic precursor migration to successive hematopoietic organs during zebrafish development. Immunity. 25(6): 963-75.

[5] Soza-Ried, C., I. Hess, *et al*. Essential role of c-myb in definitive hematopoiesis is evolutionarily conserved. Proc Natl AcadSci U S A. 107(40): 17304-8.

[6] Westerfield M. 2000. The zebrafish book. A guide for the laboratory use of zebrafish (Danio rerio). Eugene: Univ. of Oregon Press. 4.

[7] Liu, W.Y., *et al*. 2005. Efficient RNA interference in zebrafish embryos using siRNA synthesized with SP6 RNA polymerase. Development Growth and Differentiation. 47(5): 323-331.

[8] Amatruda J. F., J. L. Shepard, *et al*. 2002. Zebrafish as a cancer model system. Cancer Cell. 1(3): 229-231.

[9] Bartel. 2009. MicroRNAs: target recognition and regulatory functions. Cell. 136(2): 215-233.

[10] Beckwith L. G., J. L. Moore, *et al*. 2000. Ethylnitrosourea induces neoplasia in zebrafish (Danio rerio). Lab Invest. 80(3): 379-385.

[11] Bennett C. M., J. P. Kanki, *et al*. 2001. Myelopoiesis in the zebrafish, Danio rerio. Blood. 98(3): 643-651.

[12] Chen C. H., Y. H. Sun, *et al*. 2009. Comparative expression of zebrafish lats1 and lats2 and their implication in gastrulation movements. Dev Dyn. 238(11): 2850-2859.

[13] Hisa T., S. E. Spence, *et al*. 2004. Hematopoietic, angiogenic and eye defects in Meis1 mutant animals.EMBO Journal. 23(2): 450-459.

[14] Landthaler M., A. Yalcin, *et al*. 2004. The human DiGeorge syndrome critical region gene 8 and Its D. melanogaster homolog are required for miRNA biogenesis. Curr Biol. 14(23): 2162-2167.

[15] Lee Y., K. Jeon, *et al*. 2002.MicroRNA maturation: stepwise processing and subcellular localization. EMBO Journal. 21(17): 4663-4670.

[16] Lele, Z., P. H. Krone. 1996. The zebrafish as a model system in developmental, toxicological and transgenic research. Biotechnol Adv. 14(1): 57-72.

[17] Li, S., H. F. Moffett, *et al.* MicroRNA expression profiling identifies activated B cell status in chronic lymphocytic leukemia cells. PLoS One. 6(3): e16956.

[18] Rodriguez, A., S. Griffiths-Jones, *et al*., 2004. Identification of mammalian microRNA host genes and transcription units. Genome Res. 14(10A): 1902-1910.

[19] Romania, P., V. Lulli, *et al*. 2008. MicroRNA 155 modulates megakaryopoiesis at progenitor and precursor level by targeting Ets-1 and Meis1 transcription factors.Br J Haematol. 143(4): 570-580.

[20] Rushworth S. A. Targeting the oncogenic role of miRNA in human cancer using naturally occurring compounds. Br J Pharmacol. 162(2): 346-348.

[21] Sangokoya, C., M. J. Telen, *et al*. microRNA miR-144 modulates oxidative stress tolerance and associates with anemia severity in sickle cell disease. Blood. 116(20): 4338-4348.

[22] Sayed D., C. Hong, *et al.* 2007. MicroRNAs play an essential role in the development of cardiac hypertrophy. Circ Res. 100(3): 416-424.

[23] Zhao Y., E. Samal *et al*. 2005. Serum response factor regulates a muscle-specific microRNA that targets Hand2 during cardiogenesis. Nature. 436(7048): 214-220.